

# He-, Ne-, and Ar-Phosgene intermolecular potential energy surfaces

Cristian R. Munteanu<sup>†‡</sup>, Christian Henriksen<sup>§</sup>, Peter M Felker<sup>||</sup>, and Berta Fernández<sup>\*†</sup>

<sup>†</sup> Computer Science Faculty, University of Coruña, E-15071 A Coruña, Spain

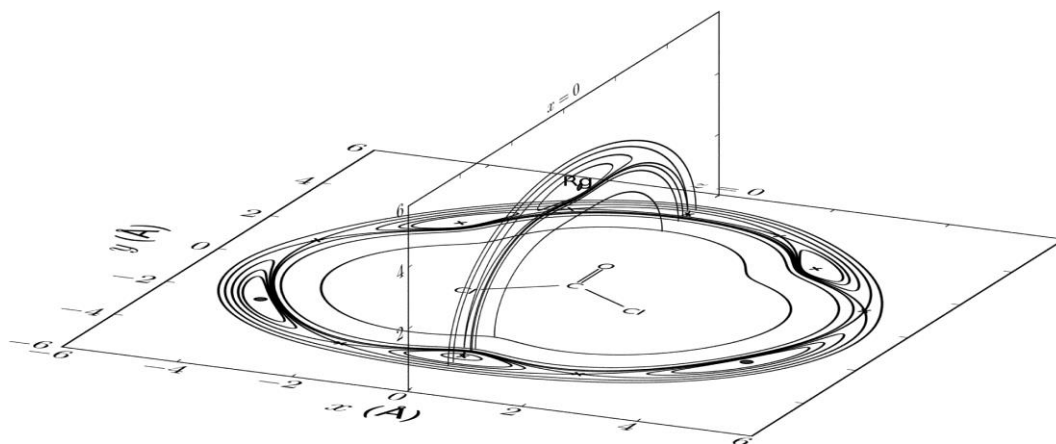
<sup>§</sup> Department of Mathematics, Technical University of Denmark, DK-2800 Kongens Lyngby, Denmark

<sup>||</sup> Department of Chemistry and Biochemistry, University of California, Los Angeles, California 90095-1569, United States

<sup>‡</sup> Department of Physical Chemistry and Center for Research in Biological Chemistry and Molecular Materials (CIQUS), University of Santiago de Compostela, E-15782 Santiago de Compostela, Spain

## Abstract

Using the CCSD(T) model, we evaluated the intermolecular potential energy surfaces of the He-, Ne-, and Ar-phosgene complexes. We considered a representative number of intermolecular geometries for which we calculated the corresponding interaction energies with the augmented (He complex) and double augmented (Ne and Ar complexes) correlation-consistent polarized valence triple- $\zeta$  basis sets extended with a set of 3s3p2d1f1g midbond functions. These basis sets were selected after systematic basis set studies carried out at geometries close to those of the surface minima. The He-, Ne-, and Ar-phosgene surfaces were found to have absolute minima of  $-72.1$ ,  $-140.4$ , and  $-326.6$   $\text{cm}^{-1}$  at distances between the rare-gas atom and the phosgene center of mass of 3.184, 3.254, and 3.516 Å, respectively. The potentials were further used in the evaluation of rovibrational states and the rotational constants of the complexes, providing valuable results for future experimental investigations. Comparing our results to those previously available for other phosgene complexes, we suggest that the results for Cl<sub>2</sub>-phosgene should be revised.



## I. INTRODUCTION

Weak molecular complexes are the focus of many studies, because they have intermolecular interaction potentials dominated by the dispersion interaction. They are used as models for studying this type of interaction,<sup>1</sup> which plays a key role in the study of processes as crucial as the solvation or adsorption of molecules.<sup>2,3</sup> Because of the importance of these phenomena in chemistry and biology, several thematic issues of *Chemical Reviews* have been dedicated to studies of these complexes.<sup>4-6</sup> Taking these factors into account, it is easy to understand the great interest in these systems, which have been extensively studied both experimentally and theoretically. From the theoretical point of view, the dispersion interaction is very demanding, regarding not only correlation method but also basis set. The high accuracy of the experimental data available increases the interest in theoretical investigations.

In previous works, we performed theoretical studies of several van der Waals complexes, evaluating highly accurate intermolecular energies using the coupled-cluster singles and doubles model including connected triples corrections [CCSD(T)] and augmented correlation-consistent polarized valence basis sets extended with sets of midbond functions. We considered both ground states<sup>7-9</sup> and singlet<sup>8,10</sup> and triplet<sup>11</sup> excited states. By fitting the intermolecular energies to analytic functions, we obtained intermolecular potential energy surfaces (IPESs). We subsequently used these surfaces used to obtain intermolecular properties, such as rovibrational energy levels and gas virial coefficients, and compared the results to the available experimental data. For the ground states, the comparison was extremely good, and it was possible to correct some of the experimental assignments. For the excited states, the agreement was slightly worse, but still satisfactory. Here, we extend this work to the He-, Ne-, and Ar-phosgene complexes. To the best of our knowledge, no experimental or theoretical results are available for these complexes. Because of the high accuracy obtained in our previous studies on weakly bonded complexes, we expect the present results to be predictive and useful for future investigations on the chemistry of these systems.

On one hand, phosgene is a toxic asphyxiating gas that causes serious damage to the human body. On the other hand, it has major industrial importance and is widely used in the fields of polymer materials, chemical agriculture, and dyes, among others.<sup>12</sup> Phosgene is generated by the photooxidation and photocatalytic oxidation of chlorinated ethenes, processes that are used to remove pollutants in industry, where improper waste treatments can cause serious contamination of the environment. The annual production of phosgene is more than 1 million tons worldwide, the majority of which is used in the manufacture of isocyanates and polyurethane and polycarbonate resins. Phosgene is also extensively used as a synthetic reagent in organic chemistry, in particular in the preparation of acyl chlorides, chloroformate esters, organic carbonates, and carbamoyl chlorides. It has also been detected in the stratosphere, mainly produced after several steps following the photolysis of CCl<sub>4</sub>, an important compound in atmospheric chemistry.

Many studies have been published on the phosgene molecule, but not that many on molecular complexes in which this unit participates. The latter can play an important role in the reduction of phosgene pollution and in the chemical industry. Therefore, it is important to carry out further theoretical studies on these systems. It is interesting to determine how phosgene interacts and to predict the intermolecular geometries of its possible complexes. Of the available theoretical studies, the majority were carried out at the Moeller-Plesset 2 (MP2) level and with rather small basis sets. In this respect, it is worth mentioning the work by Boutellier et al.<sup>13</sup> on the COCl<sub>2</sub>-chlorine complex, in which the interaction was considered both spectroscopically and theoretically. In this way, the Fermi resonances in the parent and complexed halogenated systems were quantitatively analyzed, and the structure, complexation energy, and vibrational frequencies of the complexes were calculated at the MP2 level using the 6-31G\* basis set. These results were improved by Nowek and Leszczynski,<sup>14</sup> who used the MP2, MP4, and DFT methodologies and medium-sized basis sets. The minimum-energy structure of the complex is reported to be planar with a bent conformation, characterized by an interaction with the phosgene O atom and an energy of -1.43 kcal/mol at the MP4(SDTQ)/MSPBS level, where MSPBS denotes Sadlej's polarized basis set.

The phosgene–water IPES was evaluated by Tanaka et al.<sup>15</sup> using the MP2 method and basis sets such as 6-31++G(d,p), 6-311++G(d,p), aug-cc-pVDZ, and aug-cc-pVTZ. Two non-hydrogen-bonded minima were found on the surface, one for a perpendicular structure with C $\cdots$ O and O $\cdots$ H contacts (energy = -12.46 kJ/mol) and the other coplanar with a Cl $\cdots$ O contact (energy = -8.24 kJ/mol). Significant structural differences were found with respect to the formaldehyde–water complex.

Recently, work was carried out on the COCl<sub>2</sub>-NH<sub>3</sub>, -H<sub>2</sub>S, and -PH<sub>3</sub> complexes.<sup>12</sup> The geometries of the complexes were evaluated at the MP2/aug-cc-pVTZ level. The stable structures were divided into those that interact through the phosgene C atom and those in which the interaction is through the Cl atom. The former are more stable. The interaction energy for the most stable conformer is -0.14282 eV, more stable than the COCl<sub>2</sub>-H<sub>2</sub>O system. Pavel et al.<sup>16</sup> studied the interaction of phosgene with 25 monomer clusters, using molecular dynamics simulations to predict the interaction energies, the closest intermolecular distances, and the active site groups. Only 5 of the 25 investigated systems gave stable interaction energies.

In general, the agreement between previous theoretical and experimental results is what can be expected for the MP2 method and low-quality basis sets. Considering the weakness of the interaction, higher-level correlation methods and larger basis sets are clearly needed to carry out this type of study. To the best of our knowledge, this is the first coupled-cluster investigation of IPESs in which the phosgene molecule participates.

This article is organized as follows: In section , we provide computational details for the evaluation of the interaction energies. In section , the fitting procedure is described, and the obtained IPESs are analyzed. Section is dedicated to the intermolecular level structure, and in the last section, we summarize and draw conclusions about the results.

## II INTERACTION ENERGIES

The structure of the phosgene molecule was taken from the gas electron diffraction and microwave spectroscopy study carried out by Nakata et al.<sup>17</sup> and kept fixed in all calculations. The C–O distance was set equal to 1.1785 Å, the C–Cl distance to 1.7424 Å, and the Cl–C–Cl angle to 111.83° (see Figure 1). The molecule was placed in the *xy* plane, with the C–O bond along the *y* axis and the molecular center of mass in the origin of the coordinate system. We define as intermolecular coordinates those of the vector that gives the position of the rare-gas atom with respect to the phosgene center of mass, that is, the Cartesian (*x*, *y*, *z*) components or the spherical polar coordinates (*r*,  $\theta$ ,  $\phi$ ). The interaction energies were evaluated using a supermolecular approach, within the CCSD(T) methodology. We corrected the interaction energies for basis set superposition error with the counterpoise method of Boys and Bernardi.<sup>18</sup>

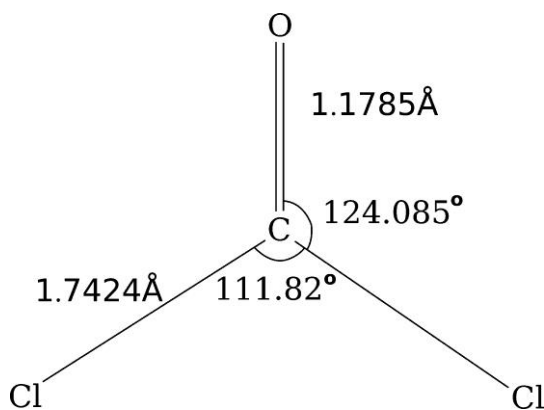


**Figure 1.** Phosgene internal coordinates.

We started the calculations by carrying out a systematic basis set selection study. For this study, we considered two intermolecular geometries close to the IPES minima, namely,  $(x, y, z) = (0.0, 0.5, 3.5)$  Å and  $(x, y, z) = (4.3, -2.3, 0.0)$  Å. We evaluated interaction energies using the series of basis sets *aug-cc-pVXZ* ( $x = s, d, t$ ;  $X = D, T, Q$ ) and the corresponding basis sets augmented with a set of *3s3p2d1f1g* midbond functions<sup>19</sup> (denoted 33211 in this article). These functions have as exponents 0.90, 0.30, and 0.10 for the *s* and the *p* functions; 0.60 and 0.20 for the *d* functions; and 0.30 for the *g* and *f* functions and are centered in the middle of the intermolecular bond. The results are presented in Table 1. Taking into account the ranges of interaction energies, we considered as error limits for the analysis 1 cm<sup>-1</sup> for the Ar and Ne complexes and 0.5 cm<sup>-1</sup> for the He complex. In all cases, the addition of midbond functions to the basis sets clearly provided an efficient means to accelerate basis set convergence. For instance, for the Ar-phosgene complex, the *aug-cc-pVXZ* energies can be estimated to converge to the value of -325.20 cm<sup>-1</sup> by using the extrapolation function  $E(x) = E_{\text{CBS}} + A \exp(-Bx)$ , where  $x = 2, 3$ , and 4 for  $X = D, T$ , and  $Q$ , respectively;  $E(x)$  is the *aug-cc-pVXZ* interaction energy;  $E_{\text{CBS}}$  is the basis-set-converged interaction energy; and  $A$  and  $B$  are adjustable parameters. We concluded that, at the quadruple- $\zeta$  level, we were still about 22 cm<sup>-1</sup> from the basis set limit result. Taking into account the *aug-cc-pVXZ-33211* results, convergence was reached much faster, already at the triple- $\zeta$  level. With respect to augmentation, the *aug-cc-pVTZ-33211* basis set in the case of the He complex and the *aug-cc-pVTZ-33211* basis set for the Ne and Ar complexes were saturated with respect to further extensions. In all cases, triple augmentation was not needed.

**Table 1.** Interaction Energies (in cm<sup>-1</sup>) Used in the Basis Set Selection Study<sup>a</sup>

| geometry              | $(x, y, z) = (0.0, 0.5, 3.5)$ Å |         |         | $(x, y, z) = (4.3, -2.3, 0.0)$ Å |         |        |
|-----------------------|---------------------------------|---------|---------|----------------------------------|---------|--------|
|                       | aug-                            | daug-   | taug-   | aug-                             | daug-   | taug-  |
| COCl <sub>2</sub> -He |                                 |         |         |                                  |         |        |
| cc-pVDZ               | -44.03                          | -46.15  | -46.33  | -22.76                           | -24.87  | -25.11 |
| cc-pVTZ               | -51.91                          | -54.26  |         | -30.21                           | -32.55  |        |
| cc-pVDZ-33211         | -57.52                          | -57.66  | -57.64  | -32.51                           | -32.76  |        |
| cc-pVTZ-33211         | -56.77                          | -57.08  |         | -34.74                           | -35.10  |        |
| cc-pVQZ-33211         | -56.89                          |         |         |                                  |         |        |
| COCl <sub>2</sub> -Ne |                                 |         |         |                                  |         |        |
| cc-pVDZ               | -73.42                          | -95.47  | -96.23  | -30.99                           | -49.11  | -49.86 |
| cc-pVTZ               | -77.95                          | -114.31 |         | -58.91                           | -69.53  |        |
| cc-pVDZ-33211         | -114.64                         | -119.17 |         | -70.37                           | -75.13  |        |
| cc-pVTZ-33211         | -115.70                         | -119.27 | -119.72 | -69.89                           |         |        |
| cc-pVQZ-33211         | -117.52                         |         |         |                                  |         |        |
| COCl <sub>2</sub> -Ar |                                 |         |         |                                  |         |        |
| cc-pVDZ               | -181.74                         | -199.72 |         |                                  |         |        |
| cc-pVTZ               | -269.02                         | -293.41 |         | -101.19                          | -124.70 |        |
| cc-pVQZ               | -303.17                         |         |         |                                  |         |        |
| cc-pVDZ-33211         | -330.74                         | -335.37 |         | -144.12                          | -147.50 |        |
| cc-pVTZ-33211         | -322.14                         | -326.43 | -326.90 | -154.06                          |         |        |
| cc-pVQZ-33211         | -322.76                         |         |         |                                  |         |        |

<sup>a</sup> See text for notation.

With the selected basis sets, we evaluated 461, 509, and 416 interaction energies for the He, Ne, and Ar complexes, respectively. The interaction energy results are included in the Supporting Information.

### III. INTERMOLECULAR POTENTIAL ENERGY SURFACES

It is very convenient to fit interaction energy data to relatively simple expressions, because then the fits can be used to compute properties of the complexes. This strategy has been used many times in the literature. Because the primary use of the fits is in simulations, it is important that the fitting function can be computed quickly; is precise, especially in the low-energy region; and continues to behave in a physically reasonable manner when the distance between the rare-gas atom and the phosgene molecule tends to either zero or infinity. We found a function satisfying these requirements using a many-body expansion with exponential terms.

We denote the position vector of the rare-gas atom as  $\mathbf{x}$  and the positions of the phosgene atoms as  $\mathbf{a}_j$  ( $j = 1-4$ ), where  $j = 1$  corresponds to C,  $j = 2$  to O, and  $j = 3$  and 4 to the two Cl atoms. Let

$$x_j(x) = k \exp\left(\frac{-\|\mathbf{x} - \mathbf{a}_j\|}{s}\right), j = 1 - 4 \quad (1)$$

with  $k = 10$ .  $s$  is a fitting coefficient, and the constant  $k$  is purely cosmetic and ensures that the coefficients of the fit are roughly comparable. Then, we fit to a polynomial  $F \in R[x_1, x_2, x_3, x_4]$  on which we imposed symmetry in the distance to the two Cl atoms. We forced symmetry by taking  $F$  to be a linear combination of terms of the form

$$\frac{1}{2} x_1^\alpha x_2^\beta (x_3^{\gamma_1} x_4^{\gamma_2} + x_3^{\gamma_2} x_4^{\gamma_1}) \quad (2)$$

This means our polynomial takes the form

$$F(x) = \sum \frac{c^{\alpha, \beta, \gamma_1, \gamma_2}}{2} x_1^\alpha x_2^\beta (x_3^{\gamma_1} x_4^{\gamma_2} + x_3^{\gamma_2} x_4^{\gamma_1}) \quad (3)$$

where the sum runs over a set of four-tuples of integers  $(\alpha, \beta, \gamma_1, \gamma_2)$ .

These terms are many-body terms, that is, functions of the distances between the atoms. If we let  $n$  denote the number of nonzero indexes, then

$$\frac{c^{\alpha, \beta, \gamma_1, \gamma_2}}{2} x_1^\alpha x_2^\beta (x_3^{\gamma_1} x_4^{\gamma_2} + x_3^{\gamma_2} x_4^{\gamma_1}) \quad (4)$$

is a sum of two  $(n + 1)$ -body terms.

Because we are especially interested in obtaining a good fit when the interaction energy is low, we defined weights  $w_i$  and minimized the expression

$$\sum_i w_i^2 [E_i - F(x_i)]^2 \quad (5)$$

where we let

$$w_i = \frac{1}{E_i - E_{\min}} \quad (6)$$

Here,  $E_{\min}$  could be the minimum interaction energy; however, in practice, we simply let  $E_{\min}$  equal the smallest computed ab initio value of the energy,  $-1 \text{ cm}^{-1}$ . Even though the weighting diminished the impact of extreme energies, we discarded points with a calculated interaction energy exceeding  $1000 \text{ cm}^{-1}$ .

For the He complex, we computed 454 interaction energies lower than  $1000\text{ cm}^{-1}$ , found the fit (i.e., those which terms to include in the function), and determined the corresponding coefficients. For the best fit among the functions that behaved physically reasonably near the phosgene molecule, the square root of the sum of weighted squared errors was equal to 0.0022. The unweighted mean square error was  $0.4051\text{ cm}^{-1}$ . Considering only points where the ab initio energy was negative, the unweighted mean square error dropped to  $0.0863\text{ cm}^{-1}$ , conforming to the fact that we placed large weights on points with low energies. Numerical calculations indicated that the fit had global minima of  $-72.14\text{ cm}^{-1}$  at the geometries  $(0, 0.6170, \pm 3.1240)\text{ \AA}$  and local minima of  $-35.23\text{ cm}^{-1}$  at  $(\pm 4.2286, -2.2827, 0)\text{ \AA}$ . As far as we could tell, there were no other minima.

Fitting the Ne- and Ar-phosgene data to the same type of function gave similar results (see Table 2). For Ne (Ar), we computed 474 points (384 points) with energies lower than  $1000\text{ cm}^{-1}$ . The main stationary points are given in Table 2.

**Table 2.** IPES Fitting Errors (rms) and Main Stationary Points, Given by Their Interaction Energies and Intermolecular Geometries

|  | $\text{COCl}_2\text{-He}$  | $\text{COCl}_2\text{-Ne}$  | $\text{COCl}_2\text{-Ar}$  |
|--|----------------------------|----------------------------|----------------------------|
| weighted rms error                         | 0.0021965                  | 0.0022464                  | 0.0017140                  |
| rms error ( $\text{cm}^{-1}$ )             | 0.4051                     | 0.7334                     | 0.6567                     |
| rms error for $E < 0$ ( $\text{cm}^{-1}$ ) | 0.0863                     | 0.1448                     | 0.2878                     |
| abs min $E$ ( $\text{cm}^{-1}$ )           | -72.1                      | -140.4                     | -326.6                     |
| abs min geometry ( $\text{\AA}$ )          | $(0, 0.6170, \pm 3.1240)$  | $(0, 0.5860, \pm 3.2006)$  | $(0, 0.5161, \pm 3.4778)$  |
| local min $E$ ( $\text{cm}^{-1}$ )         | -35.2                      | -74.1                      | -182.4                     |
| local min geom ( $\text{\AA}$ )            | $(\pm 4.2286, -2.2827, 0)$ | $(\pm 4.2619, -2.3004, 0)$ | $(\pm 4.4733, -2.3940, 0)$ |

These results are quite different from those in ref 14, where the  $\text{Cl}_2$ -phosgene complex was shown to have absolute planar minima with the interaction through the O atom, with the  $\text{Cl}_2$  molecule oriented with the oxygen lone pairs. The corresponding interaction energy was about  $500\text{ cm}^{-1}$ . In the rest of the studied phosgene complexes,<sup>12,15</sup> the results were closer to ours, with global minima where the interaction was above and below the phosgene plane. For example, for the water-phosgene complex, in the global minimum, the water molecule is perpendicular to the phosgene plane, and there are coplanar local minima where the water O atom interacts with the Cl atoms.<sup>13</sup> For the rare-gas complexes, the distances between the rare-gas atoms and the C and O atoms at the absolute minima are larger than those in the case of the water complex (for example, for the He complex, the distances to the C and O atoms are 3.126 and 3.302  $\text{\AA}$ , respectively, whereas for the O atom in water, the distances are 2.825 and 2.896  $\text{\AA}$ , respectively). The planar minima in the rare-gas-phosgene complexes are also formed because of the interactions of the rare-gas atoms and the Cl atoms, and again, because of the weaker interactions, the distances between the rare-gas atoms and the Cl atoms are larger than the  $\text{O}\cdots\text{Cl}$  distance in the water complex (for instance, 3.325 versus 2.973  $\text{\AA}$  in the case of the He complex).

Both in the present study, where the phosgene interacts with rare-gas atoms, and in available studies for complexes where phosgene interacts with polar molecules,<sup>12,15</sup> the absolute minima are always characterized by an interaction through the phosgene C atom. Therefore, we believe that the theoretical results of ref 14 should be revised. To support this conclusion, we evaluated CCSD(T)/aug-cc-pVTZ-33211 interaction energies at the geometry given in ref 14 as the most stable one and at other intermolecular arrangements with the  $\text{Cl}_2$  molecule in the  $zy$  plane and parallel to the  $y$  axis. We found that, for example, the configuration where the  $\text{Cl}_2$  center of mass is located at  $(0.0000, -0.4839, 3.5375)\text{ \AA}$  is more stable than the absolute minima reported in ref 14.

Plots of the He, Ne, and Ar-phosgene IPESs are given in Figures 2–4, respectively. We plot level curves of the IPESs along with markers at the positions of the stationary points where the interaction energy is negative. For each complex, we show contour plots in the molecular plane ( $xy$ ), in a perpendicular  $xz$  plane, and in the  $yz$  plane. Considering the plots in the  $xy$  plane, it seems that a pair of points are local minima rather than saddle points, for example, those at  $(\pm 3.0889, 2.8820, 0.0)$  Å for He. If we restrict ourselves to planar configurations of the complexes, then these points are local minima; however, when nonplanar configurations are taken into account, they become saddle points. This is illustrated in the contour plots in Figures 2b–4b, which were made in planes perpendicular to the  $xy$  plane and going through the points in question.

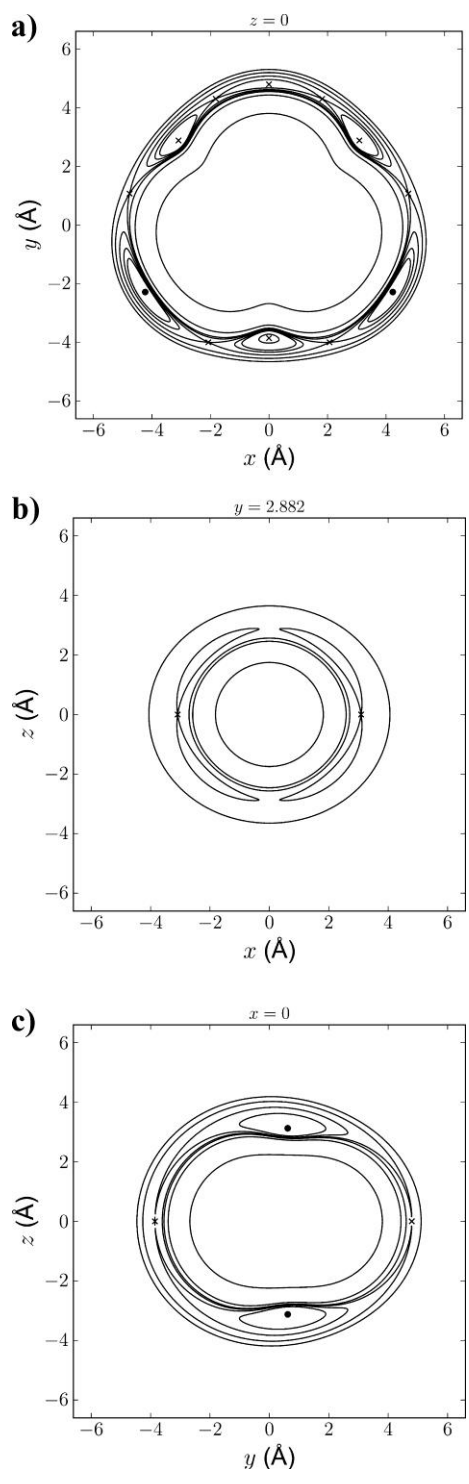


**Figure 2.** Contour plots of the He-phosgene IPES. Saddle points are marked with crosses, and minima are marked with circles. (a) In the  $xy$  plane. The plotted energy levels are  $-90.92$ ,  $-89.92$ ,  $-64.08$ ,  $-63.13$ ,  $-61.10$ ,  $-55.59$ ,  $-30$ ,  $0$ , and  $1000 \text{ cm}^{-1}$ . (b) In the plane  $y = 2.882 \text{ Å}$ . The plotted energy levels are  $-89.92$ ,  $-50$ ,  $0$ , and  $1000 \text{ cm}^{-1}$ . (c) In the  $yz$  plane. The plotted energy levels are  $-130$ ,  $-100$ ,  $-90.92$ ,  $-64.08$ ,  $-50$ ,  $0$ , and  $1000 \text{ cm}^{-1}$ .



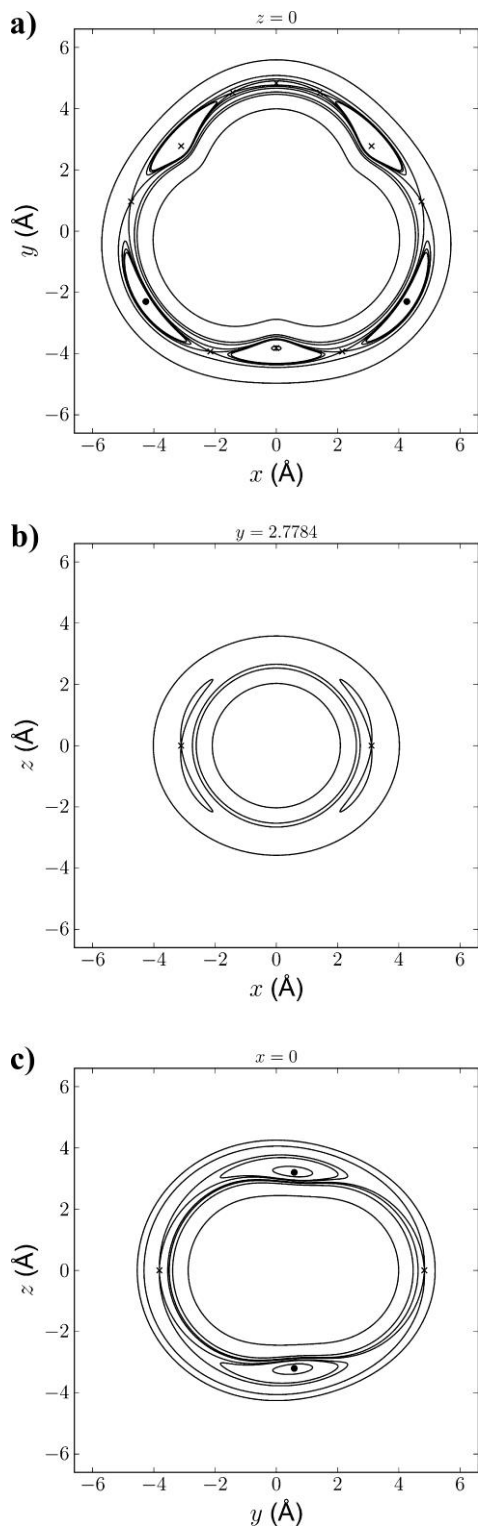


**Figure 3.** Contour plots of the Ne-phosgene IPES. Saddle points are marked with crosses, and minima are marked with circles. (a) In the  $xy$  plane. The plotted energy levels are  $-90.92$ ,  $-89.92$ ,  $-64.08$ ,  $-63.13$ ,  $-61.10$ ,  $-55.59$ ,  $-30$ ,  $0$ , and  $1000 \text{ cm}^{-1}$ . (b) In the plane  $y = 2.7784 \text{ Å}$ . The plotted energy levels are  $-89.92$ ,  $-50$ ,  $0$ , and  $1000 \text{ cm}^{-1}$ . (c) In the  $yz$  plane. The plotted energy levels are  $-130$ ,  $-100$ ,  $-90.92$ ,  $-64.08$ ,  $-50$ ,  $0$ , and  $1000 \text{ cm}^{-1}$ .

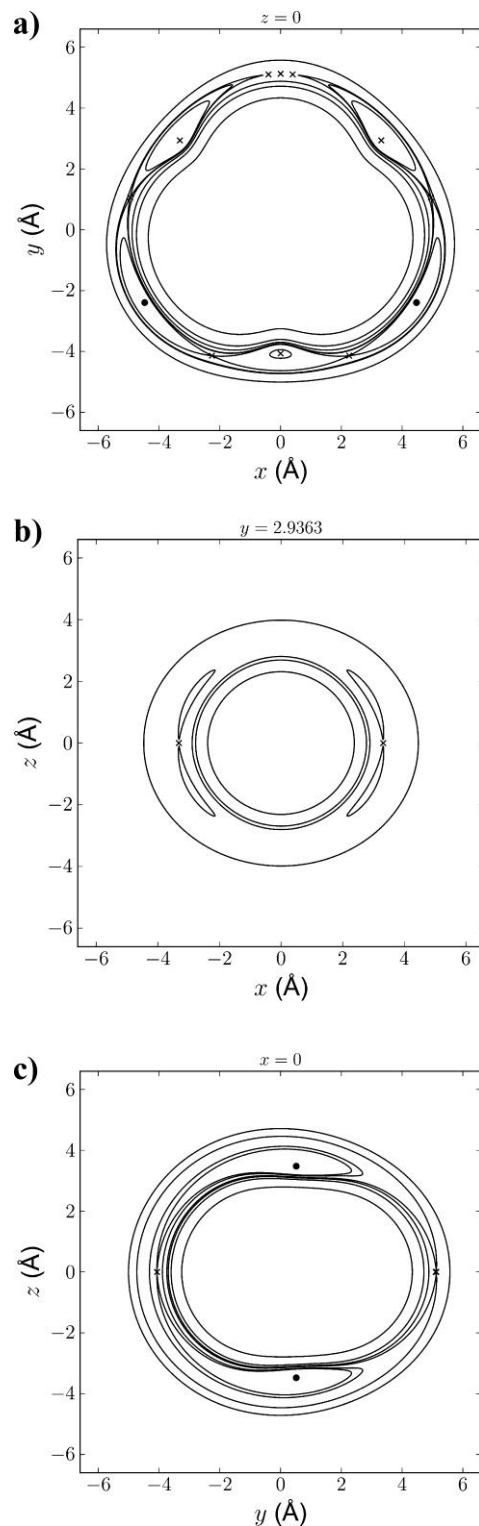


**Figure 4.** Contour plots of the Ar-phosgene IPES. Saddle points are marked with crosses, and local minima are marked with circles. (a) In the  $xy$  plane. The plotted energy levels are  $-220.96$ ,  $-211.26$ ,  $-151.16$ ,  $-138.24$ ,  $-136.00$ ,  $-100$ ,  $0$ , and  $1000 \text{ cm}^{-1}$ . (b) In the plane  $y = 2.9363 \text{ Å}$ . The plotted energy levels are  $-211.3$ ,  $-100$ ,  $0$ , and  $1000 \text{ cm}^{-1}$ . (c) In the  $yz$  plane. The plotted energy levels are  $-220.96$ ,  $-200$ ,  $-136.00$ ,  $-100$ ,  $0$ , and  $1000 \text{ cm}^{-1}$ .

#### IV. INTERMOLECULAR LEVEL STRUCTURE

Calculations of the intermolecular level structures of the He-, Ne-, and Ar-phosgene complexes employing the IPESs presented in the preceding section were carried out using procedures that we described in detail elsewhere.<sup>20</sup> Briefly, the intermolecular Hamiltonian in the rigid-monomer approximation is expressed in a three-dimensional Gauss-Hermite discrete variable representation (DVR) basis corresponding to the three Cartesian coordinates of the rare-gas atom measured with respect to the  $xyz$  axis system of section . The Hamiltonian is diagonalized in the low-energy region by filter diagonalization<sup>21,22</sup> to produce both eigenvalues and eigenvectors. For all of the species, we considered the  $^{16}\text{O}^{12}\text{C}^{35}\text{Cl}_2$  phosgene isotope, taking its mass to be 97.9368 amu and its moments of inertia along the  $x$ ,  $y$ , and  $z$  axes to be 63.82086, 145.436197, and 209.51049  $\text{amu}\cdot\text{\AA}^2$ , respectively.<sup>23</sup> For the masses of the rare-gas atoms we used 4.0026, 19.99244, and 39.98 amu for He, Ne, and Ar, respectively.

The results presented in this section are for calculations pertaining to “one-sided” complexes, in which the rare-gas atom is assumed to undergo negligible tunneling from one side of the phosgene plane to the other. We also performed two-sided calculations to assess the validity of this assumption. We found the one-sided approximation to be good for all but the highest-energy He and Ne results given herein. The molecular symmetry group of the one-sided species was found to be isomorphic to  $C_s$ . The intermolecular states were classified as either  $A'$  or  $A''$  according to whether they were symmetric or antisymmetric with respect to reflection through the  $yz$  plane.

The DVR basis sets employed were all of dimensions  $N_x \times N_y \times N_z = 40 \times 40 \times 40$ . The  $x$  DVR in each case covered the range from  $-6.5$  to  $+6.5$   $\text{\AA}$ , and the  $y$  DVR covered the range from  $-5.9839$  to  $+7.0161$   $\text{\AA}$ . The  $z$  DVR for the He complex ranged from 0.1 to 6.5  $\text{\AA}$ . For the Ne and the Ar complexes, it ranged from 0.6 to 6.6  $\text{\AA}$ .

Tables 3–5 present the intermolecular results for the He, Ne, and Ar complexes, respectively. We note several points concerning these results. First, the difference between the ground-state energy and the energy of the IPES minimum (44.0  $\text{cm}^{-1}$  for He-phosgene, 37.5  $\text{cm}^{-1}$  for Ne-phosgene, and 46.6  $\text{cm}^{-1}$  for Ar-phosgene) was found to be an appreciable fraction of the binding energy for each species, especially for the He complex. Second, large-amplitude motions, as reflected in the values of  $\Delta x$ ,  $\Delta y$ , and  $\Delta z$ , and in contour plots of the intermolecular wave functions, became prevalent at very low excitation energies for the Ne and especially the He complexes. Indeed, even for the Ar complex, the wave function excursions in the  $x$  and  $y$  directions were in the range of 1  $\text{\AA}$ , even for low-lying states. Third, as a consequence of the large-amplitude nature of the intermolecular states and the low symmetry of the complexes, assignments of the states in terms of excitations of vibrational modes is generally tenuous. We ventured some such assignments based on the presence of clear nodal planes in the intermolecular wave functions. Thus, as one can see from the wave function contour plots in Figure 5, all three species' lowest-lying excited state can be assigned to  $v_x$ , representing one quantum in the intermolecular bending mode involving motion of the rare-gas atom parallel to the  $x$  axis. Where  $v_y$  appears in the tables, it is meant to represent a state with a clear nodal plane nearly parallel to the  $xz$  plane, at least in the spatial region corresponding to large wave function amplitude. Figure 6 shows contour plots for one such state,  $N = 3$  for Ne-phosgene. Similarly,  $v_{yz}$  represents an excitation giving rise to a nodal surface that is tilted with respect to the  $y$  and  $z$  axes. An example is  $N = 4$  for Ar-phosgene, a contour plot for which is shown in Figure 7. We give these “assignments” to provide some rough idea of the nature of the states involved. We emphasize, however, that virtually all of the states were highly mixed and not amenable to facile labeling. The interested reader is directed to the Supporting Information, wherein we present contour plots of the first 10, 12, and 12 lowest-energy wave functions of the He, Ne, and Ar complexes, respectively.

**Table 3.** Calculated Characteristics of the Lowest-Energy Intermolecular States of He–Phosgene

| $N$ | $\Gamma^a$ | $\Delta E^b$ | $\langle z \rangle^c$ | $\Delta z^d$ | $\langle y \rangle^c$ | $\Delta y^d$ | $\Delta x^d$ | assignment    |
|-----|------------|--------------|-----------------------|--------------|-----------------------|--------------|--------------|---------------|
| 1   | A'         | 0.00         | 3.42                  | 0.39         | 0.80                  | 0.81         | 0.73         | ground state  |
| 2   | A''        | 9.61         | 3.12                  | 0.61         | 1.66                  | 0.91         | 1.75         | $v_x$         |
| 3   | A'         | 10.13        | 3.18                  | 0.64         | 0.96                  | 1.85         | 1.34         | $v_y$         |
| 4   | A'         | 13.25        | 2.88                  | 0.85         | -0.23                 | 2.52         | 1.70         |               |
| 5   | A''        | 15.88        | 2.49                  | 0.99         | 2.05                  | 1.40         | 2.45         |               |
| 6   | A'         | 15.96        | 2.47                  | 0.93         | -0.68                 | 2.87         | 1.80         | $(2v_y)$      |
| 7   | A'         | 18.16        | 2.61                  | 0.92         | 1.56                  | 2.78         | 2.02         |               |
| 8   | A''        | 18.67        | 2.69                  | 1.03         | -1.21                 | 1.82         | 3.40         | $(v_x + v_y)$ |
| 9   | A'         | 19.07        | 2.60                  | 1.23         | 0.34                  | 2.57         | 2.34         |               |
| 10  | A'         | 19.83        | 2.20                  | 0.94         | -0.59                 | 2.53         | 3.63         |               |

<sup>a</sup> Irreducible representation of  $M(C_s)$  to which the state belongs.

<sup>b</sup> Energy difference (in  $\text{cm}^{-1}$ ) from the ground state at  $-28.10 \text{ cm}^{-1}$ .

<sup>c</sup> Expectation value of  $z$  (in  $\text{\AA}$ ). Similarly,  $\langle y \rangle$  is the expectation value of  $y$  (in  $\text{\AA}$ ).

<sup>d</sup> Root-mean-square (rms) value (in  $\text{\AA}$ ) of  $z$ , computed as  $[(z^2) - \langle z \rangle^2]^{1/2}$ . Analogous definitions apply to  $\Delta y$  and  $\Delta x$ .

**Table 4.** Calculated Characteristics of the Lowest-Energy Intermolecular States of Ne–Phosgene

| $N$ | $\Gamma$ | $\Delta E^a$ | $\langle z \rangle$ | $\Delta z$ | $\langle y \rangle$ | $\Delta y$ | $\Delta x$ | assignment   |
|-----|----------|--------------|---------------------|------------|---------------------|------------|------------|--------------|
| 1   | A'       | 0.00         | 3.29                | 0.18       | 0.61                | 0.49       | 0.40       | ground state |
| 2   | A''      | 13.80        | 3.25                | 0.21       | 0.95                | 0.51       | 0.82       | $v_x$        |
| 3   | A'       | 15.19        | 3.28                | 0.21       | 0.56                | 0.94       | 0.57       | $v_y$        |
| 4   | A'       | 22.00        | 3.21                | 0.29       | 0.74                | 1.07       | 1.02       | $v_{yz}$     |
| 5   | A''      | 25.15        | 3.06                | 0.34       | 1.34                | 0.82       | 1.35       | $v_x + v_y$  |
| 6   | A'       | 27.27        | 3.17                | 0.36       | 0.58                | 1.37       | 1.02       | $2v_y$       |
| 7   | A'       | 30.51        | 2.99                | 0.51       | 1.17                | 1.20       | 1.46       |              |
| 8   | A''      | 31.61        | 2.87                | 0.58       | 1.37                | 1.10       | 1.69       |              |
| 9   | A'       | 32.56        | 3.13                | 0.45       | -0.50               | 1.76       | 0.54       |              |
| 10  | A'       | 34.15        | 2.90                | 0.70       | 1.21                | 1.26       | 1.60       |              |
| 11  | A''      | 35.62        | 2.78                | 0.78       | 1.29                | 1.21       | 1.83       |              |
| 12  | A'       | 36.79        | 2.56                | 0.75       | -1.38               | 2.19       | 0.86       |              |
| 13  | A'       | 38.63        | 2.44                | 0.87       | 1.15                | 1.88       | 1.95       |              |
| 14  | A''      | 40.02        | 2.78                | 0.77       | 1.62                | 1.00       | 1.78       |              |
| 15  | A''      | 40.28        | 2.93                | 0.74       | 1.20                | 1.33       | 1.56       |              |
| 16  | A'       | 41.65        | 2.63                | 0.84       | -0.63               | 2.46       | 0.82       |              |

<sup>a</sup> Energy difference (in  $\text{cm}^{-1}$ ) from the ground state at  $-102.90 \text{ cm}^{-1}$ . Other symbols have the same meaning as in Table 3.

**Table 5.** Calculated Characteristics of the Lowest-Energy Intermolecular States of Ar-Phosgene

| $N$ | $\Gamma$ | $\Delta E^a$ | $\langle z \rangle$ | $\Delta z$ | $\langle y \rangle$ | $\Delta y$ | $\Delta x$ | assignment      |
|-----|----------|--------------|---------------------|------------|---------------------|------------|------------|-----------------|
| 1   | A'       | 0            | 3.52                | 0.13       | 0.52                | 0.40       | 0.30       | ground state    |
| 2   | A''      | 21.63        | 3.51                | 0.14       | 0.71                | 0.41       | 0.58       | $v_x$           |
| 3   | A'       | 22.86        | 3.51                | 0.14       | 0.48                | 0.72       | 0.36       | $v_y$           |
| 4   | A'       | 34.68        | 3.54                | 0.19       | 0.46                | 0.69       | 0.52       | $(v_{yz}/2v_x)$ |
| 5   | A''      | 41.88        | 3.48                | 0.16       | 0.83                | 0.69       | 0.76       | $v_x + v_y$     |
| 6   | A'       | 42.30        | 3.50                | 0.18       | 0.81                | 0.56       | 0.72       | $(v_z/2v_x)$    |
| 7   | A'       | 46.43        | 3.53                | 0.18       | 0.38                | 0.87       | 0.43       | $(v_z)$         |
| 8   | A'       | 52.40        | 3.50                | 0.19       | 0.40                | 1.07       | 0.60       | $(2v_y/2v_x)$   |
| 9   | A''      | 52.75        | 3.49                | 0.21       | 0.70                | 0.75       | 0.87       |                 |
| 10  | A'       | 57.61        | 3.41                | 0.23       | 0.89                | 0.97       | 1.03       |                 |
| 11  | A''      | 60.14        | 3.44                | 0.28       | 0.97                | 0.71       | 1.05       |                 |
| 12  | A''      | 64.06        | 3.48                | 0.17       | 0.91                | 0.77       | 0.80       |                 |
| 13  | A'       | 65.52        | 3.50                | 0.24       | -0.02               | 1.27       | 0.52       |                 |
| 14  | A'       | 68.04        | 3.39                | 0.30       | 0.93                | 0.98       | 1.11       |                 |
| 15  | A''      | 68.66        | 3.35                | 0.34       | 1.06                | 0.92       | 1.25       |                 |
| 16  | A'       | 69.20        | 3.46                | 0.31       | 0.53                | 1.12       | 0.88       |                 |

<sup>a</sup> Energy difference (in  $\text{cm}^{-1}$ ) from the ground state at  $-280.02 \text{ cm}^{-1}$ . Other symbols have the same meaning as in Table 3.

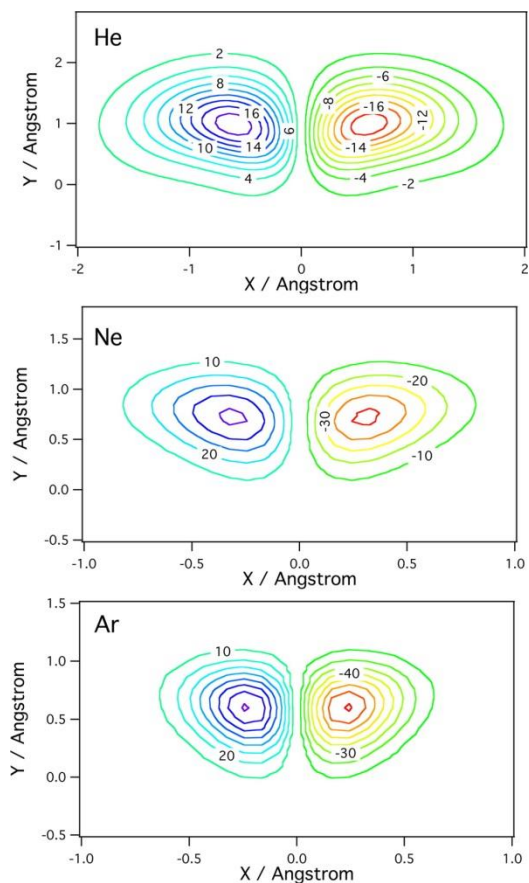


**Figure 5.**  $xy$  contour plots of the calculated  $N = 2$  intermolecular vibrational wave functions of (top) He-phosgene at  $z = 3.26$  Å, (middle) Ne-phosgene at  $z = 3.45$  Å, and (bottom) Ar-phosgene at  $z = 3.5625$  Å. Each state is assigned as  $\nu_x$  of the species. Units are arbitrary.

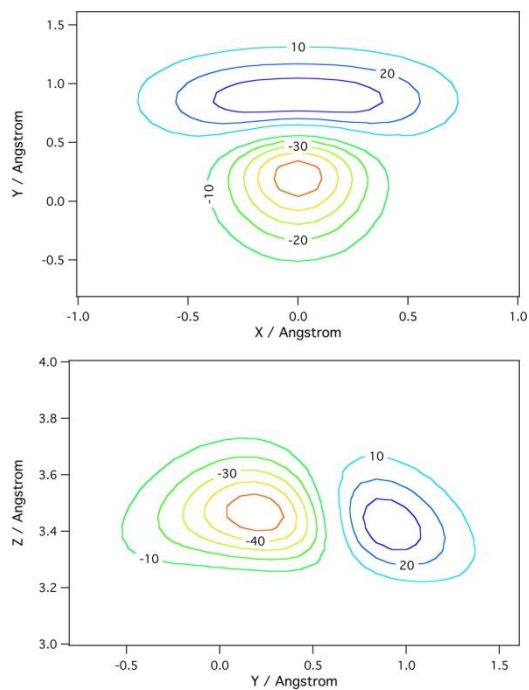


**Figure 6.** Contour plots of the calculated  $N = 3$  intermolecular vibrational wave function of Ne-phosgene assigned as  $\nu_y$ . (Top) The  $xy$  plot corresponds to  $z = 3.4125$  Å. (Bottom) The  $yz$  plot corresponds to  $x = 0$ . Units are arbitrary.

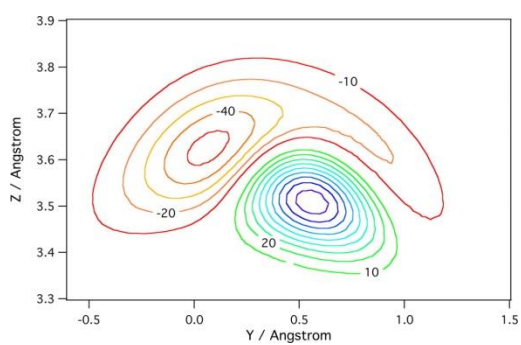


**Figure 7.**  $yz$  contour plot ( $x = 0$ ) of the calculated  $N = 4$  intermolecular vibrational wave function of Ar-phosgene assigned as  $\nu_{yz}$ . Units are arbitrary.

In addition to intermolecular vibrational energies, we also computed principal rotational constants for the ground states of the complexes by making use of the Eckart method described elsewhere.<sup>20</sup> The results are given in Table 6. We expect that these results might prove valuable in any experimental search for the rotational transitions of the species.

**Table 6.** Calculated Ground-State Rotational Constants (in  $\text{cm}^{-1}$ ) for the Rare-Gas–Phosgene Complexes

| rare-gas atom | <i>A</i> | <i>B</i> | <i>C</i> |
|---------------|----------|----------|----------|
| He            | 0.1500   | 0.09032  | 0.07851  |
| Ne            | 0.083    | 0.068    | 0.049    |
| Ar            | 0.0819   | 0.0394   | 0.0329   |

## V. SUMMARY AND CONCLUSIONS

Accurate ground-state IPESs were obtained for the He–, Ne–, and Ar–phosgene complexes. For the evaluation of the interaction energies, we used the CCSD(T) method, and after systematic basis set studies, we selected the aug-cc-pVTZ-33211 basis set in the case of the He complex and the daug-cc-pVTZ-33211 basis set for the Ne and Ar complexes. We chose 461, 509, and 416 representative intermolecular geometries for the He, Ne, and Ar complexes, respectively, to carry out the calculations. We fit the energies to analytic functions that allow quick and accurate fits, especially in the region with low energy, that behave in a physically reasonable manner when the distances between the complex fragments tend to either zero or infinity. This was accomplished by using a many-body expansion with exponential terms.

The He–, Ne–, and Ar–phosgene surfaces were found to be characterized by absolute minima of  $-72.1$ ,  $-140.4$ , and  $-326.6 \text{ cm}^{-1}$  at distances between the rare-gas atom and the phosgene center of mass of 3.184, 3.254, and 3.516 Å, respectively. We evaluated the intermolecular level structure of the complexes, obtaining valuable results for future experimental investigations. Considering the present results and those previously available for other phosgene complexes,<sup>12-15</sup> we believe that the theoretical results for the  $\text{Cl}_2$ –phosgene complex (ref 14 and references cited therein) should be revised by carrying out calculations at a higher correlation level and using larger basis sets.

### Acknowledgment

This work was supported by the Ministerio de Ciencia e Innovación, the Xunta de Galicia, and FEDER (Projects CTQ2008-01861/BQU, CTQ2011-29311-C02-01, and INCITE09 314 252 PR). We acknowledge computing time from CESGA. C.R.M. thanks the Isidro Parga Pondal Program from Xunta de Galicia and the European Social Fund (ESF).

## References

- (1) Weber, Th.; Riedle, E.; Neusser, H. J.; Schlag, E. W. Van der Waals Bond Lengths and Electronic Spectral Shifts of the Benzene–Kr and Benzene–Xe Complexes *Chem. Phys. Lett.* 1991, 183, 77–83
- (2) Leutwyler, S.; Bösiger, J. Rare-Gas Solvent Clusters: Spectra, Structures, and Order–Disorder Transitions *Chem. Rev.* 1990, 90, 489–507
- (3) Weber, Th.; Neusser, H. J. Structure of the Benzene–Ar<sub>2</sub> Cluster from Rotationally Resolved Ultraviolet Spectroscopy *J. Chem. Phys.* 1991, 94, 7689–7699
- (4) Michl, J.; Gladysz, J. A., Eds. *Chem. Rev.* 1986, 86, 491–657.
- (5) Michl, J.; Zahradnik, R., Eds. *Chem. Rev.* 1988, 88, 815–988.
- (6) Castleman, A. W., Jr.; Hobza, P., Eds. *Chem. Rev.* 1994, 94, 1721–2160.
- (7) Koch, H.; Fernández, B.; Christiansen, O. The Benzene–Argon Complex: A Ground and Excited State *ab Initio* Study *J. Chem. Phys.* 1998, 108, 2784–2790
- (8) Koch, H.; Fernández, B.; Makarewicz, J. Ground State Benzene–Argon Intermolecular Potential Energy Surface *J. Chem. Phys.* 1999, 111, 198–204
- (9) Lee, S.; Romascan, J.; Felker, P. M.; Pedersen, T. B.; Fernández, B.; Koch, H. Study of the Benzene–N<sub>2</sub> Intermolecular Potential-Energy Surface *J. Chem. Phys.* 2003, 118, 1230–1241
- (10) Fernández, B.; Koch, H.; Makarewicz, J. Benzene–Argon S<sub>1</sub> Intermolecular Potential Energy Surface *J. Chem. Phys.* 1999, 111, 5922–5928
- (11) López Cacheiro, J.; Fernández, B.; Koch, H.; Makarewicz, J.; Hald, K.; Jorgensen, P. Benzene–Argon Triplet Intermolecular Potential Energy Surface *J. Chem. Phys.* 2003, 119, 4762–4767
- (12) Bing, W. G. *Ab Initio* Complex Weak Interaction BSSE. Ph.D. Thesis, Jilin University, Jilin, China, 2006.
- (13) Boutellier, Y.; Abdelaoui, O.; Schriver, A.; Schriver-Mazzuoli, L. van der Waals Complexes between COCl<sub>2</sub>, COFCl, COF<sub>2</sub>, and Chlorine Molecule: An Infrared Matrix Isolation and *ab Initio* Study *J. Chem. Phys.* 1995, 102, 1731–1739
- (14) [
- (15) Nowek, A.; Leszczynski, J. Post-Hartree–Fock and DFT Level Studies on the Cl<sub>2</sub>CO⋯Cl<sub>2</sub> Complex: Accurate Molecular Parameters, Harmonic Vibrational Frequencies, and Interaction Energies *Int. J. Quantum Chem.* 1996, 60, 1007–1013
- (16) Tanaka, N.; Tamezane, T.; Nishikiori, H.; Fujii, T. An *ab Initio* Study of the Phosgene–Water Complex *J. Mol. Struct. (THEOCHEM)* 2003, 631, 21–28
- (17) Pavel, D.; Lagowski, J.; Jackson Lepage, C. Computationally Designed Monomers for Molecular Imprinting of Chemical Warfare Agents—Part V *Polymer* 2006, 47, 8389–8399
- (18) Nakata, M.; Kohata, K.; Fukuyama, T.; Kuchitsu, K. Molecular Structure of Phosgene as Studied by Gas Electron Diffraction and Microwave Spectroscopy: The *r*<sub>2</sub> Structure and Isotope Effect *J. Mol. Spectrosc.* 1980, 83, 105–117
- (19) Boys, S. F.; Bernardi, F. The Calculation of Small Molecular Interactions by the Differences of Separate Total Energies. Some Procedures with Reduced Errors *Mol. Phys.* 1970, 19, 553–566
- (20) Tao, F.-M.; Pan, Y.-K. *Ab Initio* Potential Energy Curves and Binding Energies of Ar<sub>2</sub> and Mg<sub>2</sub> *Mol. Phys.* 1994, 81, 507–518
- (21) Bouzón Capelo, S.; Cagide-Fajin, J. L.; Fernández, B.; Felker, P. M. The Fluorobenzene–Argon S<sub>1</sub> Excited State Intermolecular Potential Energy Surface *J. Phys. Chem. A* 2007, 111, 7876–7881
- (22) Neuhauser, D. Bound State Eigenfunctions from Wave Packets: Time→Energy Resolution *J. Chem. Phys.* 1990, 93, 2611–2616
- (23) Wall, M. R.; Neuhauser, D. Extraction, through Filter-Diagonalization, of General Quantum Eigenvalues or Classical Normal Mode Frequencies from a Small Number of Residues or a Short Time Segment of a Signal. I. Theory and Application to a Quantum Dynamics Model *J. Chem. Phys.* 1995, 102, 8011–8022
- (24) Mandelshtam, V. A.; Taylor, H. S. A Low-Storage Filter Diagonalization Method for Quantum Eigenenergy Calculation or for Spectral Analysis of Time Signals *J. Chem. Phys.* 1997, 106, 5085–5090
- (25) Phosgene moments of inertia were computed from the reported rotational constants. See:
- (26) Yamamoto, S.; Nakata, M.; Kuchitsu, K. Equilibrium Structure and Anharmonic Potential Constants of Phosgene Derived from Rotational Constants and Electron Diffraction Intensity *J. Mol. Spectrosc.* 1985, 112, 173–182